

國立臺灣大學工學院應用力學研究所



碩士論文

Institute of Applied Mechanics

College of Engineering

National Taiwan University

Master Thesis

微流晶片應用於抗癌藥物篩選及腫瘤轉移抑制之研究

**Modeling of tumor microenvironments in a  
microfluidic chip for anti-cancer/anti-migratory drug  
screening**

劉皓凱

**Hao-Kai Liu**

指導教授：胡文聰 博士

**Advisor: Andrew M. Wo, Ph.D.**

中華民國 102 年 7 月

**July, 2013**



## 致謝


兩年的時光對我的人生來說其實是一段很短的時間，甚至十年後在回想其中的兩年也許都只剩零星的一些記憶片段，但碩士班的這兩年我想我一輩子都不會忘記，任何時候回憶起來都是記憶猶新。當初剛踏入實驗室便覺得實驗室的研究氣氛深深的感染了大學剛畢業還懵懂無知的我，這正是我所嚮往的研究生生活，而在正式上課後也被跟以往不同的高深學問所震懾，認為我能夠拜讀學習這些古代學者的知識精華真是天大的榮幸，而能夠跟身旁的同學及學長姐討論交流自己學習的感想與看法更是能夠增長自己見聞的美好時光。

感謝我的指導教授胡文聰老師，兩年來不僅提供了我良好的實驗工作場所及完整的訓練，也作為一個人生的老師不斷跟我分享人生的經驗，在我迷惑的時候也只引了我正確的道路及方向，同時被老師對研究的熱忱感動，在實驗上更有動力想要追尋高深的學問，也讓我在實驗遇到挫折時能有所依靠順利度過難關。

在研究上我要感謝昌佑一開始帶領我建立研究該有的邏輯思考及實驗方法，還有清德在我最無助時提供了我方向並與提供我所有需要的幫助，不管是每週的討論或是慢慢糾正我欠缺考慮的想法及實驗步驟，這些訓練都讓我明白自己的不足也讓我在往後的研究能夠更謹慎節省了很多時間。感謝實驗室夥伴：建明、昌佑、貞伶、清德、畊兆、清德、書聖、維遠、正偉、偉豪、存超、沛晟、聖毅、韋凡、孟澤、冠瑄，有大家的陪伴及幫助才能讓我在兩年內順利完成碩士學業，特別感謝聖毅這位好戰友，不管在修課或是在實驗室後的生活都讓我不會感到孤單能夠一起奮鬥，還有書聖讓我眼界更加遼闊，人生必須符合中庸之道，太緊湊或是太放鬆都會適得其反，但實際看到書聖的生活我才了解何謂中庸之道，讓我的人生能夠走的更穩健更踏實。

最後最重要的是感謝我的家人，沒有家人在背後的支持我一定沒辦法撐到最後一步，這個碩士學位我最想要跟我家人一同分享，希望我能成為他們的驕傲，同時他們也是我最大的榮耀。

## 中文摘要



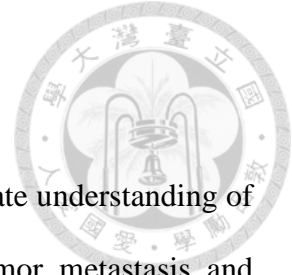
體外測試模型能夠協助研究者了解癌症轉移的發展過程同時能夠幫助釐清化療藥物是否具有治癒癌症的效果。此篇論文提出了一個微流晶片能夠用來在體外模擬觀察三維的癌症細胞轉移過程以及用做化療藥物的篩選。本實驗使用了兩種不同類型的人類乳癌細胞(MCF7, MDA-MB-231)，並且進一步將癌細胞培養呈球形以求更接近癌症在體內的真實形體來進行實驗, 利用癌症細胞外皮生長因子的趨向性來達到癌症轉移的現象。

此微流晶片包含了三層流道，最上層是兩條平行的流道用以置放癌細胞及上皮生長因子，下層的流道則佈滿了 collagen 用以模擬人體內的細胞外間質，而在中間則以一層薄膜隔開，同時薄膜上有數個小洞用以作為細胞轉移及物質擴散的通道。

結果顯示，三維的球型癌細胞比二維平層型的癌症細胞具備了較高的轉移能力，且同時對上皮生長因子的趨向性也較敏感，在轉移的方向上是順著較高濃度的上皮生長因子的方向轉移，而二維的轉移則是偏向隨機行無方向性的方式轉移。而在觀察癌症轉移的同時，此晶片亦可同時進行三維的癌症化療藥物測試，以求能夠篩選出能夠治療癌症且同時能夠抑制癌症轉移的化療藥物，期望未來臨床上能夠提供醫師進行癌症化療時用藥的參考。

關鍵字：癌症轉移，球形癌細胞，藥物篩選，微流晶片，體外模型

# ABSTRACT



In vitro studies of the complex tumor microenvironment facilitate understanding of tumor progression and even drug efficacy. In this study, 3D tumor metastasis and associated anti-cancer drug screening were studied in a microfluidic chip. The metastatic process was modeled by cells extravasate from spheroids composed of breast cancer cell lines (MCF7 and MDA-MB-231). These cells then migrated in response to EGF chemotaxi gradient with and without the influence of anti-cancer drugs.

The chip consists of two parallel top channels and a bottom channel sandwiching a perforated membrane patterned with micro holes. Solution exchange was driven by the pressure gradient caused by different liquid surface level.

The migration ability of tumor spheroid had been compared to the parental single cell and results showed that tumor spheroid had an upregulated EGFR expression and a higher invasive ability than parental cells. Also, an anti-cancer drug, paclitaxel, was introduced to do the drug test on tumor spheroids. The results showed that the IC50 value of tumor spheroid is larger than parental cell, suggesting that tumor spheroid acquire better drug resistance than parental cells. Furthermore, paclitaxel can also be served as an anti-migratory drug so we can obtain the inhibition of cancer metastasis result at the same time. This device enables study of 3D and 2D cell metastases and associated drug screening on tumor spheroid and might be useful for clinical study of personalized therapy.

Keywords: Metastasis, Cancer spheroid, Drug screening, Microfluidic chip, In vitro model

# Contents



致謝.....	i
中文摘要.....	ii
ABSTRACT.....	iii
CONTENTS.....	iv
LIST of FIGURES.....	vi
LIST of TABLES.....	vii
<b>1. Introduction.....</b>	<b>1</b>
<b>2. Material and Method.....</b>	<b>4</b>
2.1 Design concept of the microfluidic device.....	4
2.2 Evaporation-driven pump.....	8
2.3 Chip Fabrication.....	9
2.4 Cell lines.....	9
2.5 Spheroid culture.....	10
2.6 Chemosensitivity assay.....	10
2.7 Evaluation of tumor spheroid size.....	11
2.8 Experiment procedure.....	11
<b>3. Results and Discussion.....</b>	<b>12</b>
3.1 Characterization of evaporation-driven pump and the concentration gradient generator.....	12
3.2 In vitro microfluidic chemotaxis assay of 3D spheroids.....	15
3.2.1 Monolayer v.s. spheroid cells migration assay.....	16
3.2.2 Effect of different EGF concentration on tumor cell migration.....	19
3.2.3 Effect of different spheroid size on tumor cell migration.....	22
3.3 Anti-cancer drug screening.....	25

3.3.1 Morphology of cells.....	25
3.3.2 Drug toxicity profiles in the chip.....	27
<b>4. Conclusion.....</b>	<b>31</b>
Appendix.....	32
Biomimetic nano-cilia generate multicellular tumor spheroids.....	32
Experimental methods to study tumor cell migration.....	37
Reference.....	41



## List of Figures



Figure 1	<i>Schematics of microfluidic chip and experiment concept.....</i>	<i>6</i>
Figure 2	<i>Characterization of evaporation-driven pump and the concentration gradient generator.....</i>	<i>14</i>
Figure 3	<i>Tracking and observation of cancer cells migration.....</i>	<i>15</i>
Figure 4	<i>Comparison of monolayer and spheroid migration assay.....</i>	<i>18</i>
Figure 5	<i>The Effect of different EGF concentration on tumor cell migration.....</i>	<i>21</i>
Figure 6	<i>Effect of different spheroid size on tumor cell migration.....</i>	<i>24</i>
Figure 7	<i>The morphology of (a) MCF7 and (b) MDA-MD-231 during 24 hour drug perfusion.....</i>	<i>26</i>
Figure 8	<i>The effect of paclitaxel treatment on the area of spheroids attached on the channel.....</i>	<i>29</i>
Figure 9	<i>Drug toxicity profiles of Paclitaxel in tumor spheroid in the chip and the parental cells examined by MTT assays.....</i>	<i>30</i>
Figure 10	<i>3D spheroid culture with triblock-copolymer (nano-cilia)-based locomotion.....</i>	<i>35</i>
Figure 11	<i>Characteristics of triblock copolymers in steric repulsion.....</i>	<i>36</i>
Figure 12	<i>Experimental methods for investigating factors that influence tumor cell migration.....</i>	<i>39</i>

# List of Tables



**Table 1** *Comparison of in vitro experimental approaches  
to study tumor cell migration.....40*



# 1. Introduction

Inhibit cancer metastasis is one of the targets in curing cancer and has great effect on the survival of patients. Roughly 90% of cancer death is related to cancer metastasis<sup>1,2</sup>. Metastasis is a complex multi-step process; at the early stage of cancer metastasis, single cell will migrate from primary tumors to the blood vessel, then entering the circulatory system and then transport to other distant organs<sup>3</sup>.

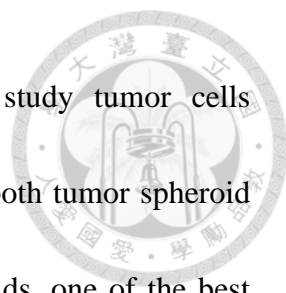
Clinically, tumors are often treated with anti-cancer drugs as a major form of treatments, for example, paclitaxel is used for breast cancer, carboplatin for lung cancer, and doxorubicin for lymphoma, etc. However, some reports have showed that when metastases occur, tumor cells will have the resistance to those anti-cancer drugs<sup>4</sup>. Hence, inhibition of cell migration might be an important goal of anti-drug treatment.

Over the past years, the research of anti-cancer drug screening and cancer cells migration are conducting separately and most anti-cancer drug screening assays is performed on cells grown as monolayer on glass or plastic platform or some surface coated with extracellular matrix (ECM). However, increasing evidence supports that three-dimensional (3D) tissue culture can exhibit the microenvironment more realistic and also obtain the more accurate corresponding of cellular morphology, cell-cell interaction, and reaction to chemical substances<sup>5,6</sup>. Some research group has also confirmed that 3D cultured cancer cells present the resistant to some anti-cancer drugs,

which are used to have great effect on two-dimensional (2D) cultured cancer cells<sup>7-11</sup>.

One common method utilized for anti-drug testing is the *in vivo* models, which might suffered from uneasy observation, high cost, moreover, even the animal models would not always present the same response to drug effect as in human body. Therefore, 3D *in vitro* model have emerged as a valuable tool to mimic the true microenvironment *in vivo* and further, to acquire more reliable result before going to animal testing.

With realization of the importance of the metastasis, scientists have developed many types of *in vitro* model to study the cell migration assay. For example, *in vitro* wound-healing assay<sup>12,13</sup>, cell exclusion zone assay<sup>14,15</sup>, microcarrier bead assay<sup>6,16</sup>, and transwell migration assay<sup>17,18</sup>. Among these assays, the transwell migration assay is the most common using for study the metastasis, and it is also called Boyden chamber assay<sup>19</sup>. The assay is composed of two medium containing chamber separated by a membrane with pores, and the cells would migrate through those pores from the upper chamber to the bottom chamber which containing some attractant. The advantages of this assay are its expediency of use, and the complex experimental facility is not necessary, however, it still exist some challenges. For instance, it is an endpoint assay, which means different cell types will have different processing time; and others like how to maintain the attractant's gradient between two chambers, the detection is difficult cause the cells are migrate in vertical direction<sup>20-22</sup>.



Herein, this paper presents a microfluidic chip that can study tumor cells migration/invasion in vitro as well as anti-cancer drugs' effect on both tumor spheroid and inhibition of tumor metastasis. The chip is suitable for spheroids, one of the best models for 3D cultures, which are spherical clusters of cells formed by self-assembly, and may attain more reliable result before the clinical treatment<sup>23-25</sup>. The chip is composed of three independent PDMS layer bonding together, to mimic the microenvironment of tumor live in-vivo, base membrane, stroma tissue, and blood vessel respectively. In addition, a stable concentration of drug and EGF is maintained by evaporation driven pump. To address the drawbacks mentioned above, we design a horizontal-migrating chip which is allowed to real-time measurement of single cell, and also simplifying the detection process.

## 2. Material and method

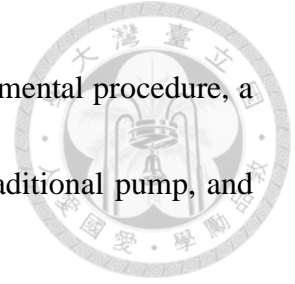


### 2.1 Design concept of the microfluidic device

In this work, we designed a microfluidic device, shown in Fig. 1, to conduct the anti-cancer drugs screening on spherical clusters of tumor cells, and the inhibition of the tumor metastasis.

The chip was composed by three single PDMS layer using O<sub>2</sub> plasma (CUTE-MP, Femto Science, Korea) bonding together. Top layer had two parallel channels to model the microenvironment *in vivo* and the human blood vessel; the bottom layer was a channel coated with collagen I to model the stroma tissue<sup>26</sup>, and the middle layer was a 10um membrane with 50um diameter micro-holes which were used for trapping cells and exchanging solutions. Tumor spheroids were loading in one of top channels and trapped by micro-holes and reagents like EGF or anti-cancer drugs were loading to another channel. Reagents would diffuse to tumor-loaded channel via bottom channel so that generating a concentration gradient within the bottom channel and once tumor cells sensed the gradient, migration and invasion would occur. The top two channels were parallel so cells would migrate in horizontal direction which facilitating the observation process.

In order to make the chip tubeless so that simplified the experimental procedure, a evaporation-driven pump (EDP) was used in chip to replace the traditional pump, and the EDP would be described below.



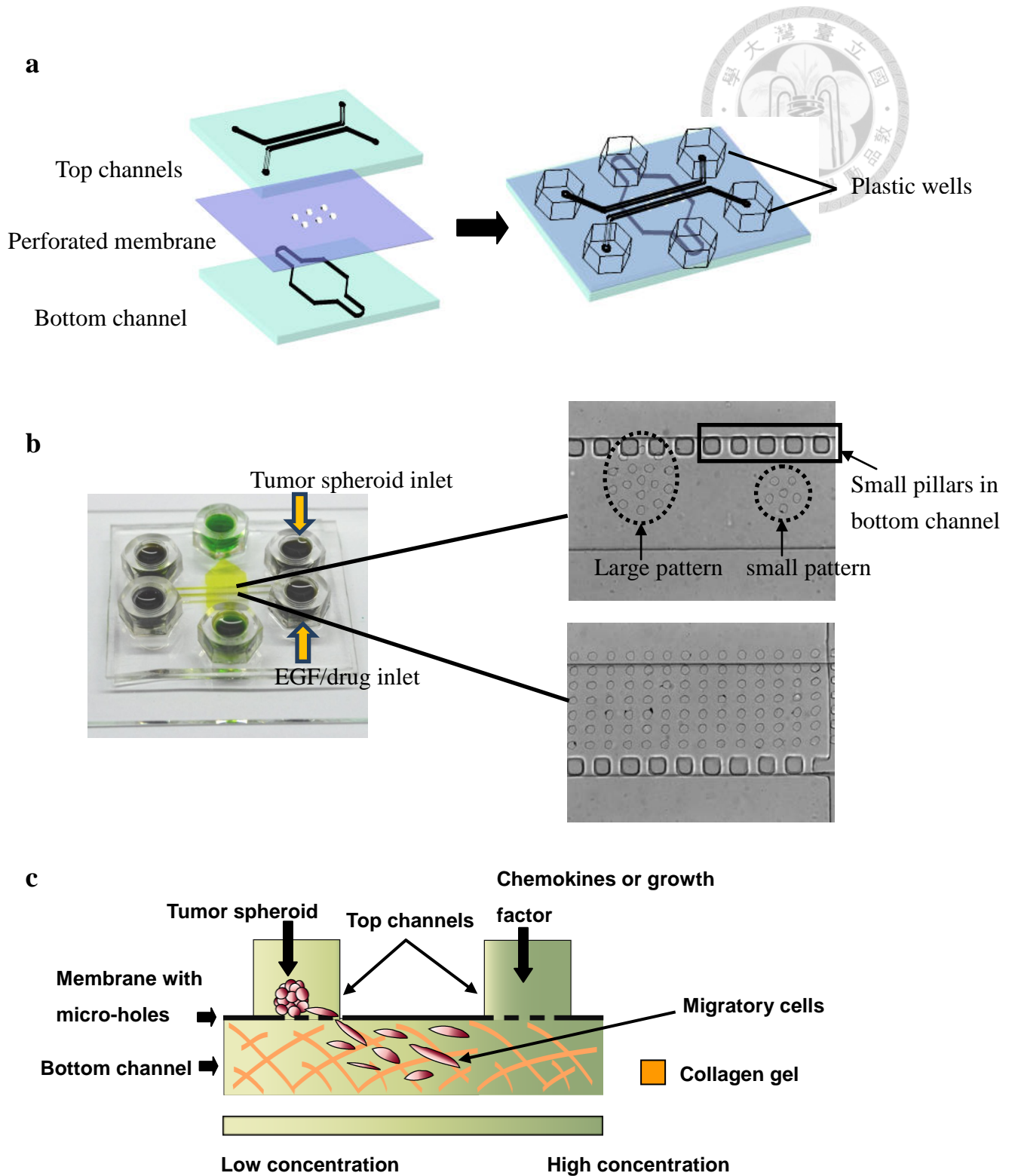
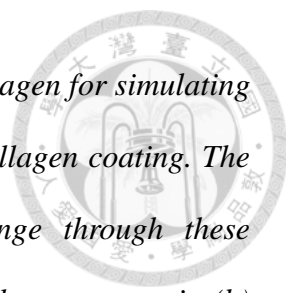


**Figure 1** (a) Schematics of our design. Our device is made of three single chips, the upper chip, the membrane in the middle, and the bottom chip. The upper chip has two channels, channel 1 is for loading primary tumor cell and channel 2 is for simulating



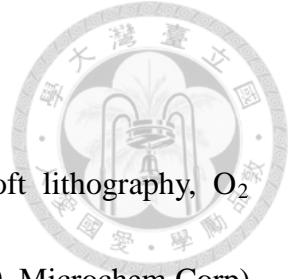
*blood vessel by loading EGF. The bottom channel is coated with collagen for simulating stroma tissue. There are some small pillars in bottom to help the collagen coating. The membrane has some microholes so the substances can exchange through these micro-holes. The channels' inlet and outlet are placed a plastic well as a reservoir. (b) The prototype of the chip, one of top channels is for loading tumor spheroid, another is for loading chemoattractant (EGF) and drugs. The spheroid-loading channel has two kind of pattern used for determine the different size of tumor spheroid. Diameter of larger pattern is 350 $\mu$ m and small pattern is 150 $\mu$ m.(c) The side view of the microfluidic chip.*



## 2.2 Evaporation-driven pump

Herein, for the purpose of maintaining a stable concentration gradient in migration zone from cell-loaded channel to blood vessel-simulated channel, we added a piece of lens paper (1 cm x 2cm) in top channels' outlets, papers were exposed to UV light overnight and full immersed in culture medium prior to locating to top channels' outlets, to increase the evaporation rate so that created a continuous flow inlet to outlet. Via refreshing the solutions in top channels, the concentration gradient in migration zone could be maintained stably for long term experiment. Simulation of a 3D time-dependent transport of species using commercial software (COMSOL Multiphysics 3.5) was conducted to facilitate the estimation of the EGF/drugs diffusion in bottom channel and 0.5 mM FITC–Dextran (FD4, Sigma) was used to visualize the operation of evaporation-driven pump. The equation  $C_s = C_0 e^{-t/\tau}$  were used to calculate the EGF/drugs concentration in the observation zone<sup>27</sup>, and  $\tau$  was defined as the source time parameter:

$\tau = (V_s h_{gel}) / (D_{avg} A_c)$ , where  $V_s$  was the volume of solution in the source,  $h_{gel}$  was the height of the gel in the port,  $D_{avg}$  was average diffusivity of the factor in solution and gel, and  $A_c$  was the limiting cross-sectional area at the channel entrance.



## 2.3 Chip Fabrication

Fabrication of the device was made of photolithography, soft lithography, O<sub>2</sub> plasma treatment and collagen coating. First, photoresist (SU-8 2050, Microchem Corp) was spin coated on a glass slide to define the microchannel pattern with desired thickness. The master was completed after developing and drying process.

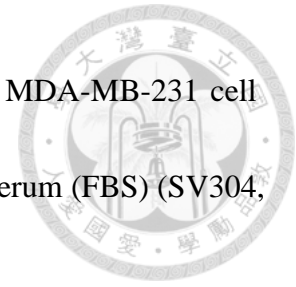
After the fabrication of master was finished, the each layer of device was formed by PDMS casting. Top and bottom channel were using A:B = 1:10 and membrane was using A:B = 1:15. Liquid PDMS was poured onto the master, while the membrane was using the spin-coater to spin coat the PDMS since its thickness was only 10  $\mu$ m, and then dried at 70°C for 1 hour to form the microchannel. Then they were treated with O<sub>2</sub> plasma and bonded together to form a closed microfluidic channel.

Type I collagen(100 $\mu$ g/ml, BD Biosciences) was first introduced into bottom and incubated at 37°C for 1 hour, and then more concentrated collagen(0.75mg/ml) was introduced into bottom and incubated at 37°C to form gel in the bottom channel.

## 2.4 Cell lines

Human breast adenocarcinoma cells, MCF7 and MDA-MD-231, were incubated in a culture dish (704001, NEST) at 37°C, 5% CO<sub>2</sub>. The culture medium were Dulbecco's modified eagle medium with nutrient mixture F12 (DMEM/F12) (12400, GIBCO) for

MCF7 cell lines and Leibovitz L-15 medium (41300, GIBCO) for MDA-MB-231 cell lines respectively. Both of them were added with 10% fetal bovine serum (FBS) (SV304, Hyclone) and 1% penicillin/streptomycin (15140, GIBCO).



## 2.5 Spheroid culture

Triblock copolymers (Pluronic F108) were prepared for spheroid culture. First, 6-cm-diameter culture dishes were exposed to UV light overnight then coated with 1% F108 for 1 h at room temperature. After washing with PBS twice, human cancer cell lines were seeded by  $2 \times 10^5$  cells with culture medium and incubated in 5% CO<sub>2</sub> incubator at 37°C. The cells were cultured for 5 to 7 days to formed spheroids and then sieved *via* a 70- $\mu$  m cell strainer (352340, BD, Franklin Lakes, New Jersey, USA) to yield spheroids larger than 70  $\mu$  m in diameter before loading to the chip. Each generation was designated by the week of cell cultures.

## 2.6 Chemosensitivity assay

The tumor spheroids were treated with Paclitaxel or Cisplatin (Bristol-Myers Squibb, Park Avenue, NY, USA) after being trapped onto micro-holes. Concentration of 1, 10, and 100 $\mu$ g/ml were chosen for the drug treatment experiments. To study the effect of the anti-cancer drugs, the area of each individual tumor spheroid spreading on

substrate was measured every 24 hours and normalized against that of untreated cells.



## 2.7 Evaluation of tumor spheroid size

The size of the 3D tumor spheroids was calculated by measuring their diameters using an imaging software (ImageJ, 1.42q). Since some spheroids were oval-shaped, the mean diameter ( $l$ ) of cell spheroids was determined by the following equation:

$l = (a \times b)^{1/2}$ , in which  $a$  and  $b$  represent two orthogonal diameters of the spheroids<sup>28</sup>.

## 2.8 Experiment procedure

The chip was exposed to UV light overnight and then loading ethanol to channels to make a sterile environment. After washing with PBS twice, the bottom channel was coated with collagen described above and one of top channel was coated with F108 to avoid cell adhering. Then tumor spheroids were loaded into the F108-coated channel and the other top channel loading with chemokines (EGF) and anti-cancer drugs (cisplatin, paclitaxel). All loading process were driven by the gravitation, by loading different liquid volume in inlet and outlet's well, the well contained more liquid would be forced to flow to the other well and complete the substances exchanging in channels.

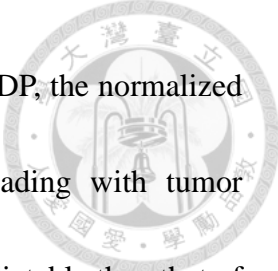
### 3. RESULTS AND DISCUSSION



#### 3.1 Characterization of evaporation-driven pump and the concentration gradient generator

Evaporation-driven pump (EDP) is characterized to ensure the ability to generate a suitable concentration gradient. The main working concept of the EDP is based on adding a piece of paper to a well to increase the liquid surface of the well so that the different evaporation rate between two wells will make a difference of liquid level to drive the flow. Therefore, the area of the paper is a key factor to generate a stable EGF/drug concentration during perfusion. The flow rate caused by the EDP should be equal to the diffusion of the solute, (diffusion coefficient of EGF in medium is  $6 \times 10^{-11} \text{ m}^2 / \text{s}^{29}$ ) or the concentration in channel will reach an equilibrium which will influence the cell migration direction. So the flow rate caused by different size of papers has been verified to ensure the ability of generating a stable concentration gradient from EDP.

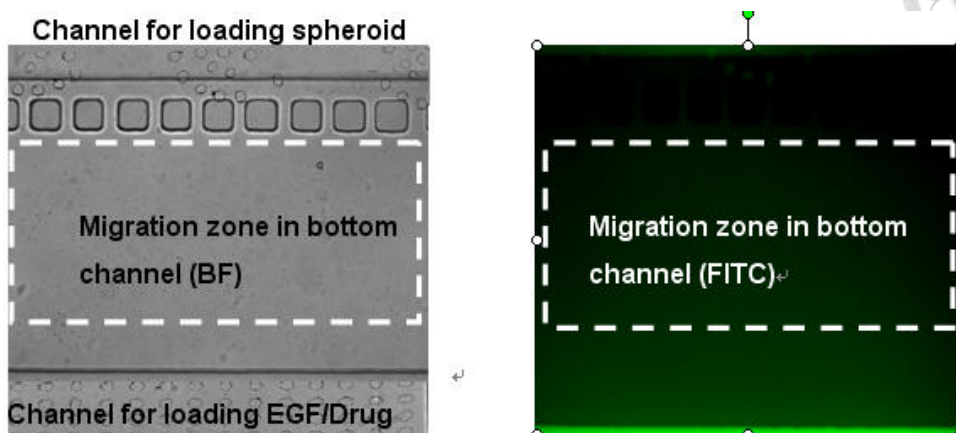
Figure 2 shows the simulation of the region for EGF/drugs diffusion in the bottom channel. Figure 2a presents the bright-field image and green fluorescent image during the operation of the EDP. The region within the dash box is the migration zone in the bottom channel. Characterization of the concentration gradient profile with or without



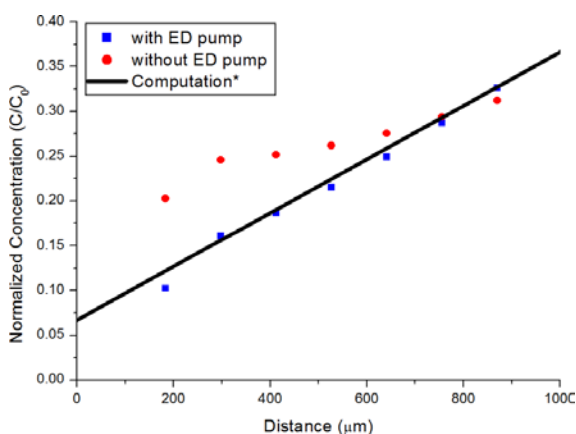
using the EDP for a long term perfusion is shown in Fig. 2b. With EDP, the normalized concentration is linear with distance away from the channel loading with tumor spheroids; without EDP, the normalized concentration is more unpredictable than that of with EDP in the forward region between 200-600  $\mu$  m. Computation result is also shown as the solid black line in the figures. The source is replenished every 24 hours and is performed by adding solution to each well to avoid drying up the channels and a long term observation had been recorded. Figure 2c shows a long term observation of EDP. The EDP can maintain a stable linear concentration gradient for 147hr, which is much longer than the whole experiment time.



**a**



**b**



**c**

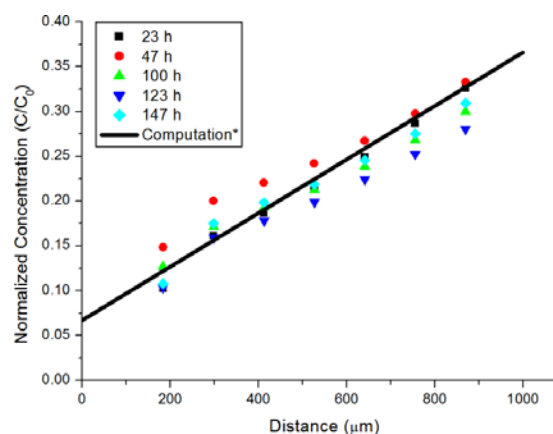


**Figure 2** Evaporation-driven pump for stable solute diffusion. (a) The bright-field (BF) images and fluorescent (FITC) images demonstrate the operation of EDP. (b) Characterization of the concentration gradient profile with or without using the ED for a long term perfusion. (c) A non-linear concentration gradient was found without the EDP, whereas a stable linear concentration gradient was acquired with the EDP



### 3.2 In vitro microfluidic chemotaxis assay of 3D spheroids

We have developed a device enable tracking the migratory cells from MCF7 (Fig 3a) and MDA-MB-231 (Fig 3b) so that we can quantify the ability of cell migration using both the cell migration rate and the numbers of migratory cells. The effect of different EGF concentration and different size of tumor spheroid have been verified.

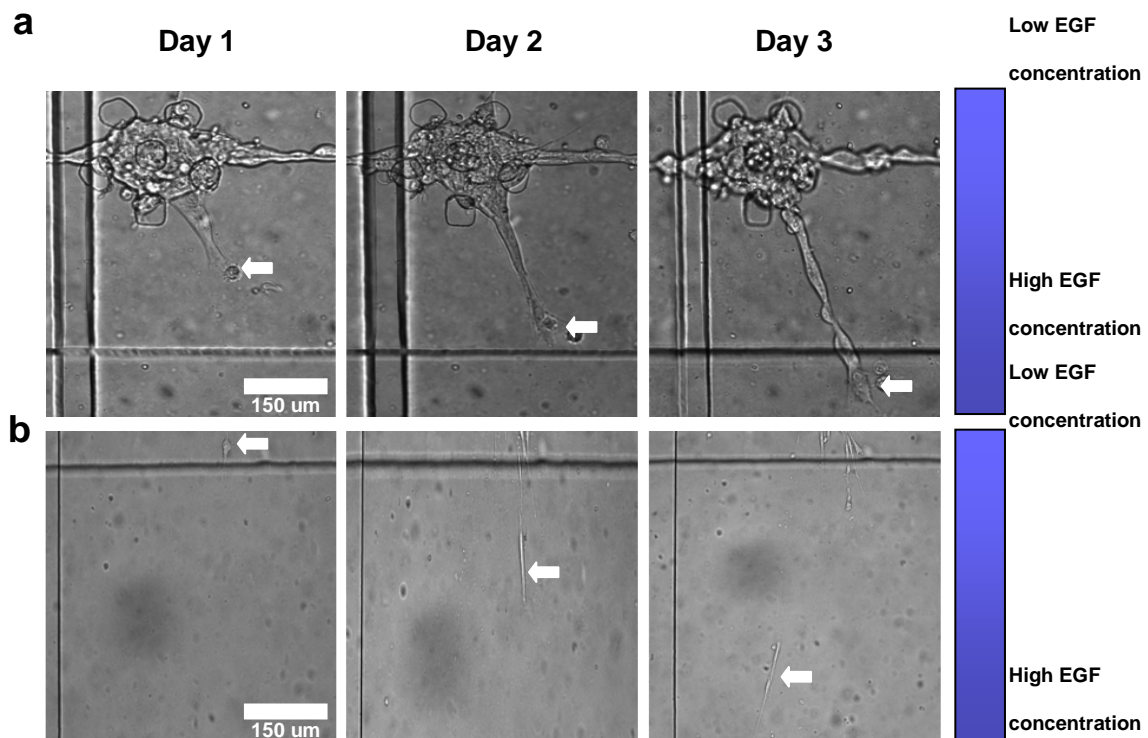



*Figure 3* The chip is enable the tracking of migratory cells. We observe the cells (a) MCF7 (b) MDA-MB-231 every 24hr and record the condition of migratory cells including the distance and numbers of migratory cells.

### 3.2.1 Monolayer v.s. spheroid cells migration assay



The experiment was performed under the same EGF concentration (50ng/ml) into the EGF channel. The cell counts and the migration rate were measured to represent the ability of migration ability of cancers. Figure 4a shows the numbers of cells migrate from spheroids and monolayer for both MCF7 and MDA-MB-231. Apparently, spheroids have larger cell counts, about 5~8 times, than monolayer cells in both MCF7 and MDA-MB-231. Figure 4b is the migration rate of cells migrating from spheroids and monolayer for both MCF7 and MDA-MB-231. The cells migrate from spheroids transported about 5 times faster than those from the monolayer. Based on the results, it may suggest that spheroids have better performance than monolayer cells in cancer migration indicating that the spheroid cells acquired an upregulated EGFR expression and a higher invasive ability than cells with a monolayer.

Migration rates of spheroids for the two cell lines (MCF7 and MDA-MB-231) which are two different typically types cancer cells (MCF7 for luminal and MDA-MB-231 for normal) are also compared the ability of cell migration. MCF7 and MDA-MB-231 are both human breast cancer cells but has different morphology where MDA-MB-231 is more mesenchymal like than MCF7. The average migration rate of all four tests is almost the same for each day which indicate that the concentration gradient



in the bottom channel is very stable so the disturbance caused by exchanging solution every 24hr is negligible. During cancer invasion and metastasis, epithelial-mesenchymal transition (EMT) plays a crucial role so MDA-MB-231 is expected to have greater invasive ability. The results (Fig 4) show that the migration rate of MDA-MB-231 spheroids (about 160 $\mu\text{m}/\text{day}$ ) is much faster MCF7 (about 50  $\mu\text{m}/\text{day}$ ) and the total numbers of cells migrate from MDA-MB-231 spheroids (51) is also larger MCF7 (32) under the same environment condition which conforming our expectation, furthermore, the migratory cells from MCF7 acquired fibroblast-like mesenchymal morphology compared to 2D culture which might suggest that these cells have undergone the EMT process.



a

	MCF7		MDA-MB-231	
	Cell count (Monolayer)	Cell count (Spheroid)	Cell count (Monolayer)	Cell count (Spheroid)
Day 1	2	10	5	15
Day 2	3	17	9	26
Day 3	3	28	9	38
Day 4	4	32	10	51

b

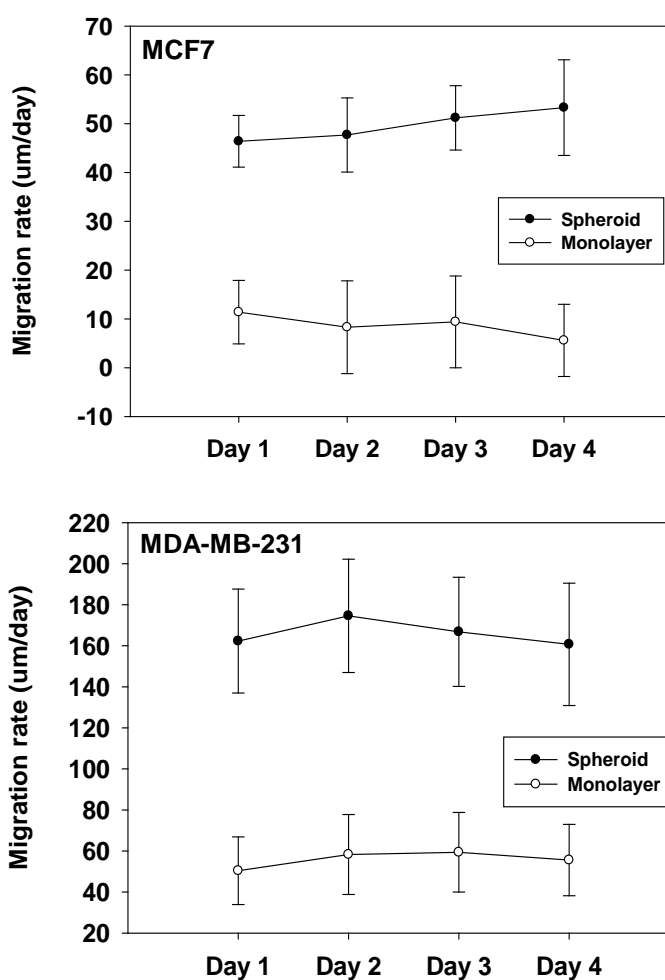
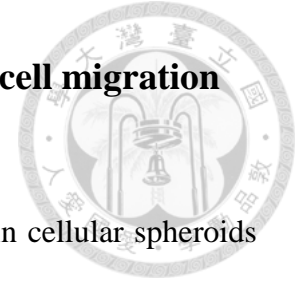


**Figure 4 Comparison of monolayer and spheroid migration assay.** (a) The migratory cell numbers observed in bottom channel. Each pattern has covered by cells so the initial cell numbers is almost the same for each pattern. (b) The average migration rate of parental and spheroid. Data (n=3) were means  $\pm$  standard deviations (SD).

### 3.2.2 Effect of different EGF concentration on tumor cell migration



Recent studies have demonstrated that EMT may be induced in cellular spheroids by some substances like epidermal growth factor (EGF). Since EGF is thought to be a governing parameter in tumor cell migration, we test two concentrations (50ng/ml and 20ng/ml) to verify the effect of EGF concentration on tumor metastasis. The culture medium is mixed with two concentrations of EGF and loading to the top channels, and the medium without EGF is served as control experiment.

Figure 5a shows the cell numbers migrating from spheroids to bottom channel. After one day EGF loading to the top channel we can observe cell migration and only very few cells migrate to bottom channel without loading EGF compare to the other two conditions, indicating that the cells migrate because of the stimulation of the EGF instead of falling down into bottom channel because of effect of gravitation. Total numbers of migratory cells of higher EGF concentration (50ng/ml) condition is almost twice the lower EGF concentration (20ng/ml condition), showing a good correlation to the EGF concentration.

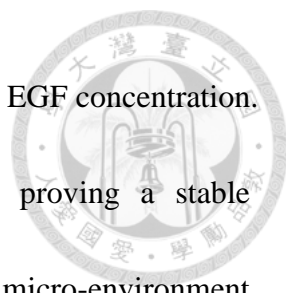
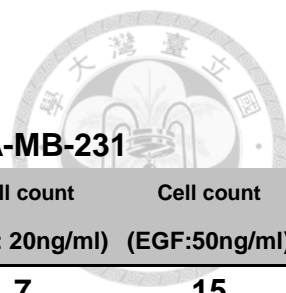


Figure 5b shows the migration rate under treating with different EGF concentration. The average migration rate is almost the same for each day proving a stable concentration gradient contained in the migration zone and a viable micro-environment for cell migration. Moreover, the stable average migration rate might indicating that the cells in the bottom are all in good condition during the whole process suggesting that this device contain a suitable environment for cell culture. This is allowed for some slowly-migrated cell types and has a potential of sorting or long term culturing the cells acquired the metastasis ability or cancer-stem-like cells' properties.

Herein, based on the results (Fig. 5), we have shown that the higher EGF concentration will lead better cancer migration performance in both MCF7 and MDA-MB-231. Meanwhile, the experiment verifies the migration ability of MDA-MB-231, including migratory cell counts and migration rate, is better than MCF7 which corresponding to the cell properties.



a

	MCF7			MDA-MB-231		
	Cell count (EGF: 0ng/ml)	Cell count (EGF: 20ng/ml)	Cell count (EGF:50ng/ml)	Cell count (EGF: 0ng/ml)	Cell count (EGF: 20ng/ml)	Cell count (EGF:50ng/ml)
Day 1	2	5	10	5	7	15
Day 2	3	8	17	9	13	26
Day 3	3	12	28	9	19	38
Day 4	4	13	32	9	26	51

b

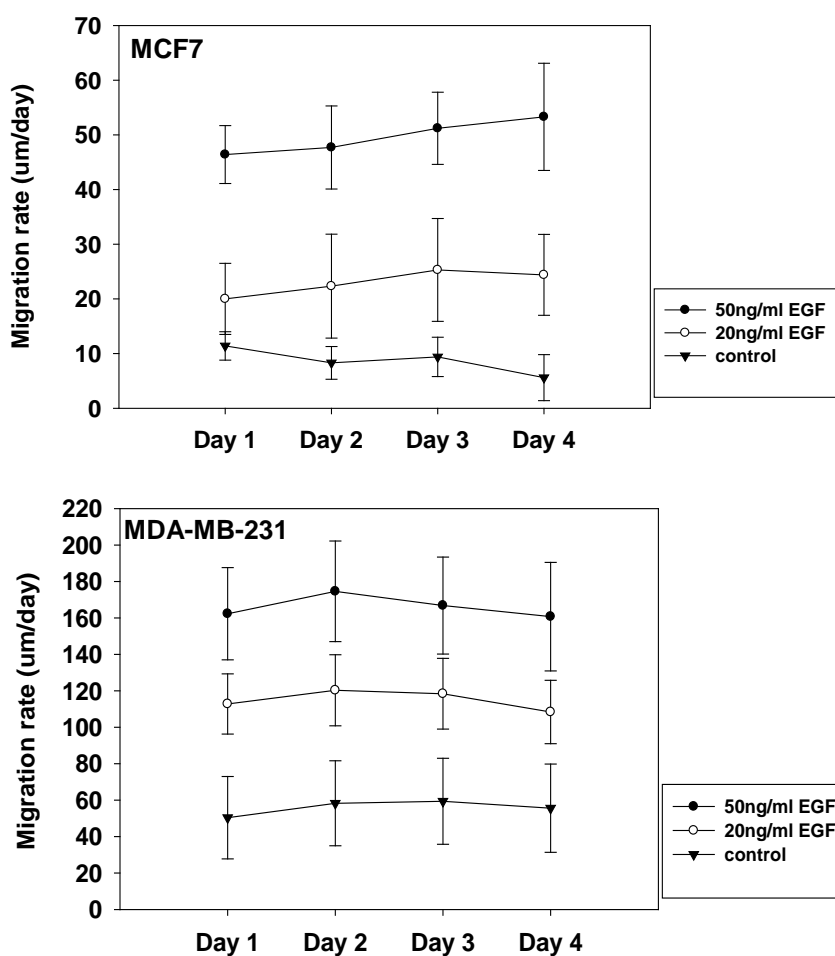
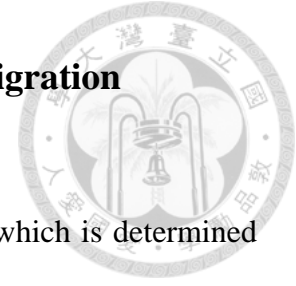


**Figure 5 The Effect of different EGF concentration on tumor cell migration.**

(a) The numbers of migratory cell under different concentration gradient (0, 20, 50ng/ml EGF). (b) The average migration rate of three conditions. Data (n=3) were means  $\pm$  standard deviations (SD).

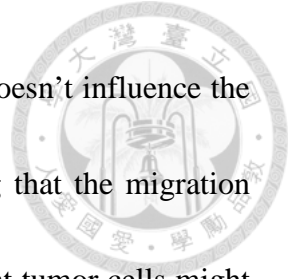
### 3.2.3 Effect of different spheroid size on tumor cell migration



The tumor spheroids are classified by the mean diameter ( $l$ ) which is determined by the following equation:  $l = (a \times b)^{1/2}$ , where  $a$  and  $b$  represent two orthogonal diameters of the spheroids. The mean diameter of loading spheroids is  $106 \pm 25 \mu\text{m}$ , so we consider the diameter smaller than  $131 \mu\text{m}$  small spheroid, and the others are large spheroids. In addition to calculate the mean diameter, the spheroids will spread and cover the whole pattern after trapping on the pattern about 2hr, so the spheroids size can also be determined by the pattern size.

The experiment were performed under the same EGF concentration (50ng/ml) introducing into the EGF channel. Figure 6a shows the MCF7 and MDA-MB-231's migratory cell numbers of different size of spheroids. Total numbers of migratory cells of larger size spheroids is about twice to small size spheroids both MCF7 and MDA-MB-231. This is corresponding to the spheroids spreading area on pattern where the large pattern's area is twice to the small pattern. So the migratory cells numbers is directly related to the local cancer cell quantity. Figure 6b presents the average migration rate of different size spheroids. The migration rate is almost the same for different size spheroids both MCF7 and MDA-MB-231

According to the results (Fig. 6), it seems the spheroid's size doesn't influence the migration rate but only the numbers of migratory cells, suggesting that the migration ability is not so related to the size of the tumors, which indicates that tumor cells might acquire the metastasis ability in early stage even during the formation of primary tumors as some research reported<sup>28,30,31</sup>.





a

	MCF7		MDA-MB-231	
	Cell count (Large spheroid)	Cell count (Small spheroid)	Cell count (Large spheroid)	Cell count (Small spheroid)
Day 1	7	4	9	6
Day 2	12	5	16	10
Day 3	19	9	25	13
Day 4	23	9	31	20

b

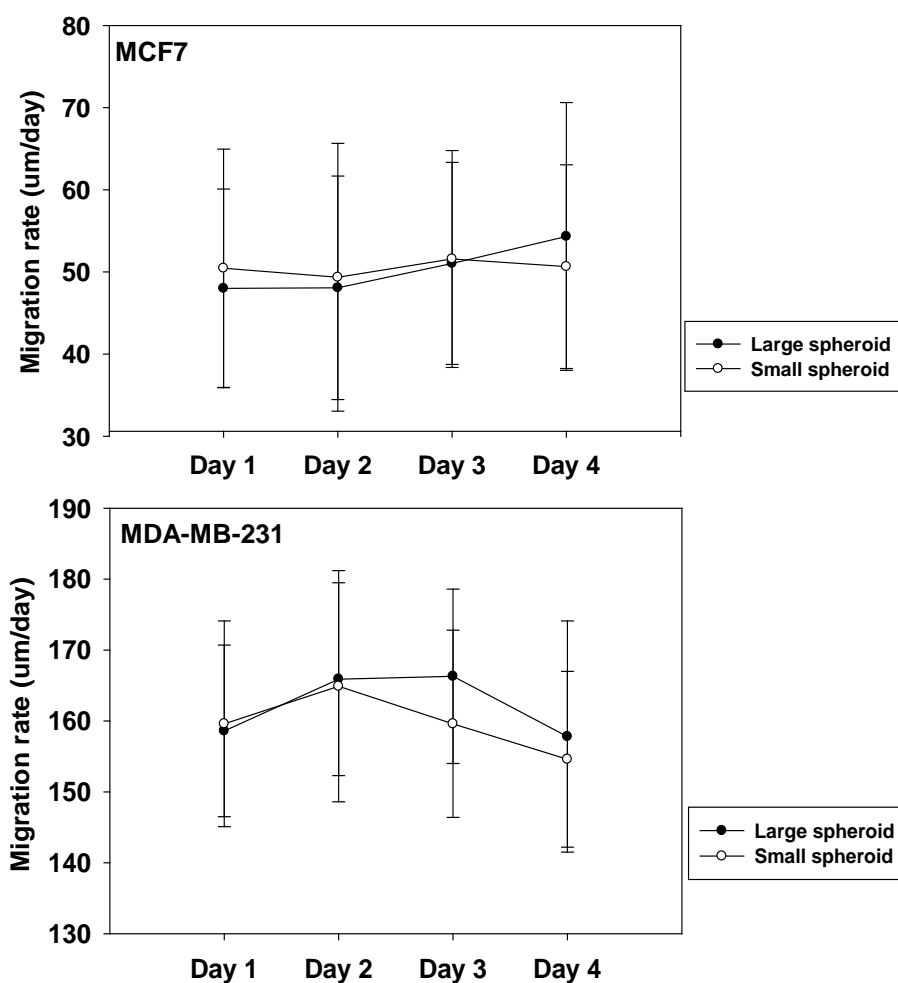


**Figure 6 Effect of different spheroid size on tumor cell migration**

(a) Migratory cell numbers of different size spheroids observed in bottom channel.

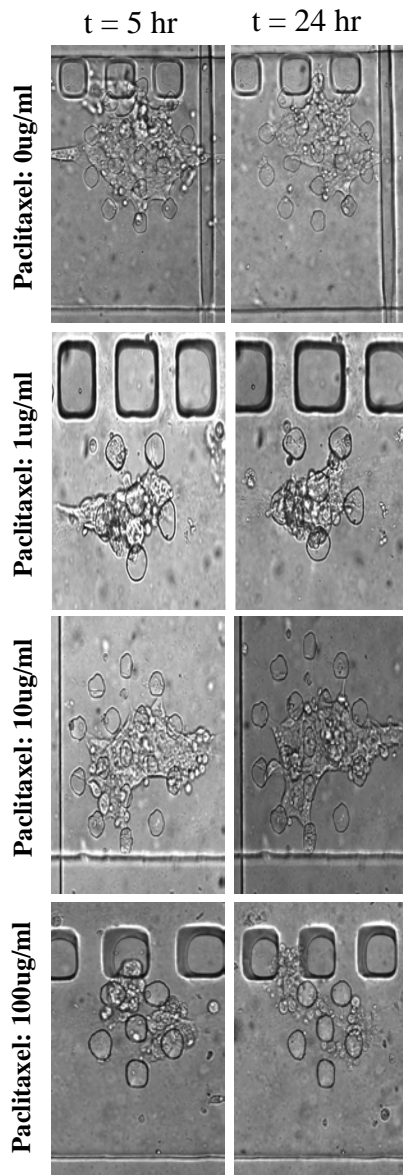
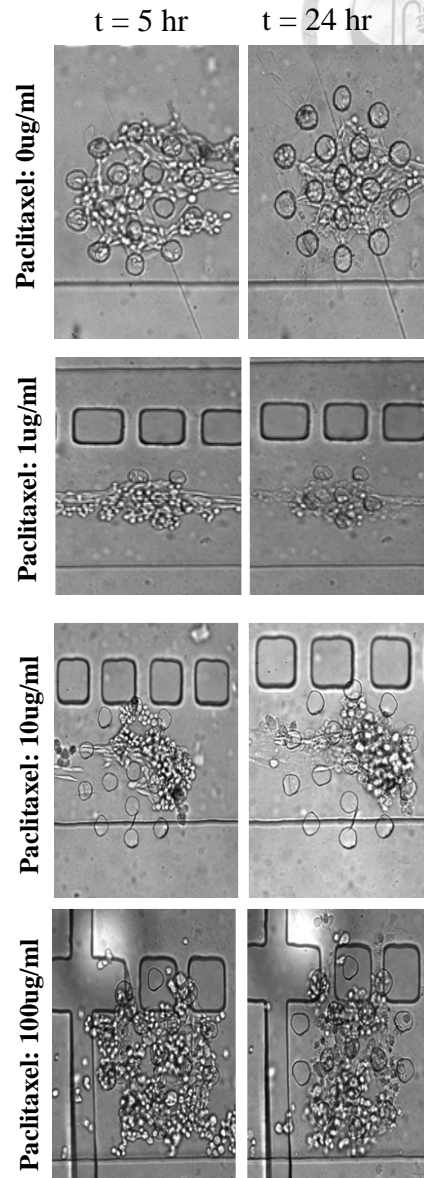
(b) The average migration rate of different size of spheroids. Data (n=3) were means  $\pm$  standard deviations (SD).

### 3.3 Anti-cancer drug screening



#### 3.3.1 Morphology of cells

The morphology of cells during 24 hour drug perfusion is shown in Fig. 7 (a. MCF7, b. MDA-MB-231). After being trapped onto the micro-holes pattern, the tumor spheroids will attach to the substrate and then grow to the surrounding areas coated with collagen. The cells without drug treatment can cover the whole micro-pattern in two days and up to 6 times the initial area in three days. But the spreading area is limited by the pattern size because only patterns are coated with collagen and the outer region of the patterns are not, so cells can't attach on it. The cell proliferation is also found in lower concentrations of drug (1  $\mu\text{g/ml}$ , 10 $\mu\text{g/ml}$ ). But the growing area is almost stop growing after drug introduce into the device. And a significant decrease in cell spreading area, due to some dead cells detaching from the substrate, were found in highest concentrations.

**a****b**

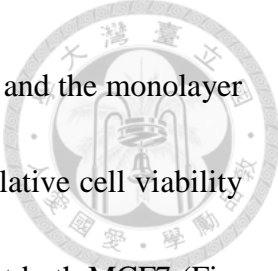
**Figure 7** Morphology of (a) MCF7 and (b) MDA-MD-231 during 24 hour drug perfusion. Tumor spheroids without or with low concentration drug treatment will attach to the substrate and then grow to the surrounding areas coated with collagen.

### 3.3.2 Drug toxicity profiles in the chip



Cell viability after drug treatment is one of the indexes of cytotoxicity. Viability of MCF-7 MMTS was examined after being treated with paclitaxel for 24hr, 48hr, and 72hr, and after 72hr, live cells and dead cells were indicated by a green dye (calthion AM) and red dye (propidium iodide).

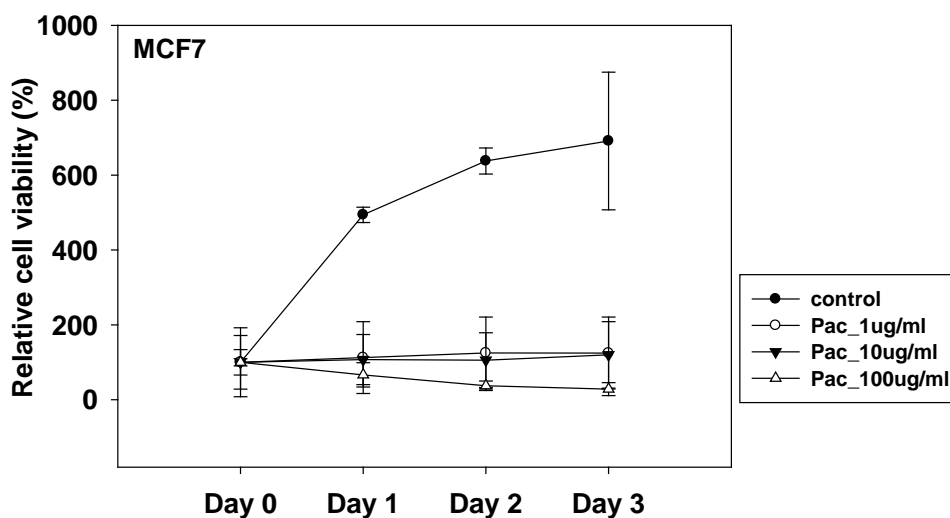
Medium was mixed with different concentrations of drug and 50ng/ml EGF then introducing into the device to conduct experiment. Reduction in tumor size is one of the positive effects from an anti-cancer drug. Herein, we measured the diameter of tumor spheroid after treated with drugs at 1, 10, 100 $\mu$ g/ml for 24hr, 48hr, and 72hr shown in Fig. 8. The growth curve is similar to the cells culture in the culture dish in monolayer forms. Relative cell viability was normalized against the untreated spheroids. The spheroids trapped on large pattern without drug treatment can grow dramatically after 72hr, whereas, the size of spheroids treated with 100 $\mu$ g/ml drug was reduced with the expansion of exposure time and the increasing of drug concentration. The cell proliferation is also found in lower concentrations of drug (1 $\mu$ g/ml, 10 $\mu$ g/ml). But the growing area is almost stop growing after drug introduce into the device.



Drug toxicity profiles of paclitaxel in tumor spheroid in the chip and the monolayer cells examined by MTT assays after 24hr are presented in Fig. 9. Relative cell viability was normalized against the untreated spheroids. The results show that both MCF7 (Fig. 9a) and MDA-MB-231 (Fig. 9b) spheroids have more resistant than monolayer cells to paclitaxel. It may prove that the malignant of cancer cells in 2D dramatically diminish and the effects of chemotherapeutic drugs or selective inhibitors employed on cell-cell communication like EMT is also reduced, whereas the behavior of cells cultured in 3D will respond more closely to *in vivo* condition<sup>32-36</sup>.



a



b

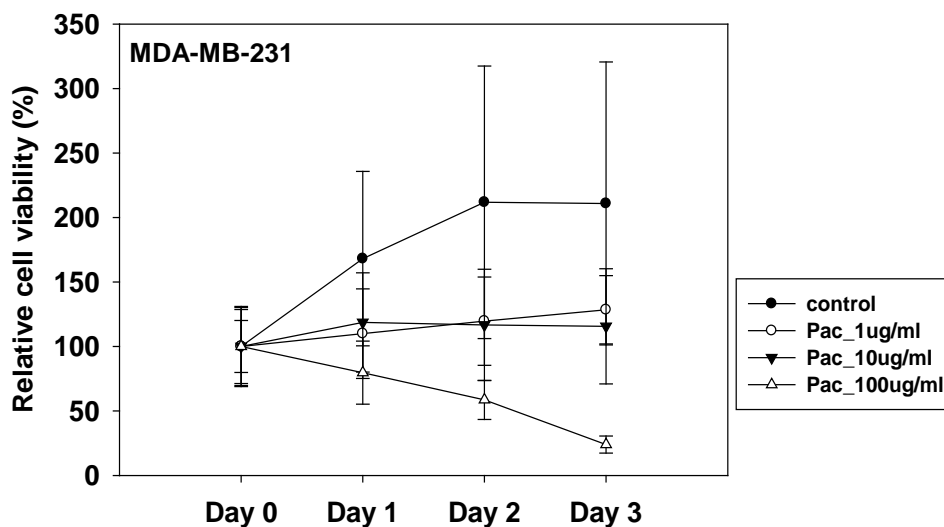
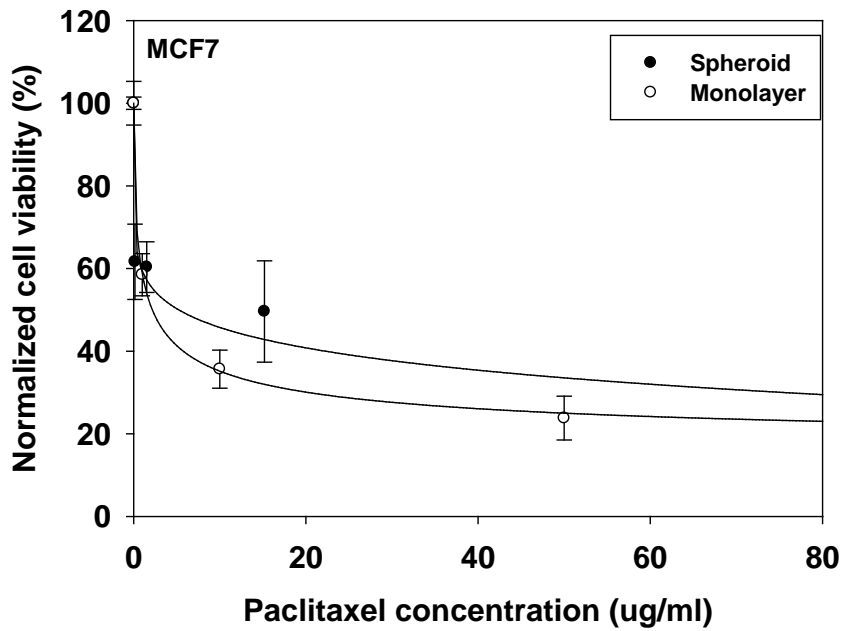


*Figure 8 Effect of paclitaxel treatment on the area of spheroids attached on the channel. The diameter of the (a) MCF-7 and (b) MDA-MB-231 spheroid reduced with an increase in exposure time (24, 48, or 72hr) and concentration (1, 10, or 100 ug/ml) of paclitaxel. The viability is normalized against the spheroid spreading area at Day 0. Data (n=3) were means  $\pm$  standard deviations (SD).*



a



b

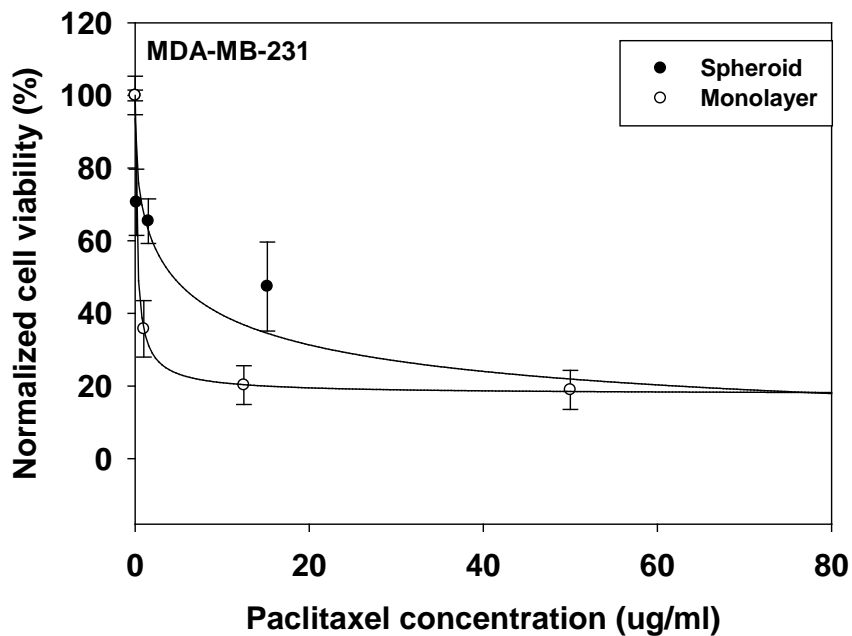
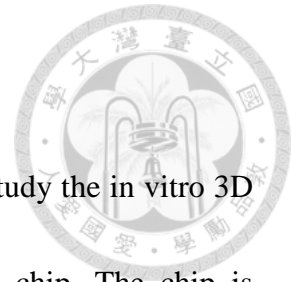


*Figure 9 Drug toxicity profiles of Paclitaxel in (a) MCF7 and (b) MDA-MB-231 spheroid in the chip and the parental cells examined by MTT assays. The viability is normalized against the spheroid spreading area at Day 0. Data (n=3) were means  $\pm$  standard deviations (SD).*

## 4. Conclusion

In summary, this work presented a microfluidic chip that can study the in vitro 3D tumor migration and the anti-cancer drug screening at the same chip. The chip is suitable for real time observation instead of endpoint assay and work as a tubeless system to facilitate the experimental process. We also demonstrate the potential of the chip for long term culture of the cells acquired metastasis ability which might be cancer-stem-like cells. In the future, the chip can be co-cultured like endothelial cell in EGF channel to better mimic blood vessel so that we can study the integrated metastasis process of tumor cell. Thus, the present device provides a viable approach to realize long term organotypic cultures that represents suitable tumor microenvironment, and may facilitate personalized drug testing.




## Appendix

### Biomimetic nano-cilia generate multicellular tumor spheroids



Figure 10a presents the methodology of 3D multicellular spheroid cultures that rely on engineered nano-cilia and cell-cell interactions, which is based on the steric repulsion of cell-to-substrate adhesion and subsequent locomotion and self-aggregation of cells into a tumor spheroid. In this study, we adopted triblock copolymer monolayer – Pluronic F108 – to as a candidate of such the biomimetic nano-cilia. Pluronic F108 is known for its nontoxicity and biocompatibility for a wide range of cellular study. It has two separated hydrophilic PEO chain lengths of 128 monomer units and a hydrophobic PPO chain length of 54 units, and the fully extending PEO chain length in solution would be approximately 45 nm, thereby it may be easily adjusted to typical cell culture platforms and micro-scale technology without interfering the microscopy observation. In addition, we have recently demonstrated that the Pluronic copolymers may be applied for the deterministic 2D/3D cell patterning by microfluidics. However, the combination of biomimetic nano cilia-mediated repulsion, locomotion, and self-aggregation to achieve 3D spheroid cultures and the subsequent phenotypic/genotypic characteristics from the resulted spheroids have not yet been systematically studied.

To first evaluate and then confirm the feasibility of triblock copolymers – coated on conventional polystyrene (PS) dishes/plates – for spheroid cultures, we applied several methodology, including multiple cell lines testing for spheroid generation, contact-angle measurement, protein repulsion, immunofluorescence detection, and long-term viability testing (Figures 10b and c, Figure 11). Figure 10b presents the



contact angle images (top panel) and the proposed schematics of the chain alignment (bottom panel). The hydrophobic PPO chains were bound onto the PS surface due to hydrophobic-hydrophobic interaction, and then the flexible and hydrophilic PEO chains were swung freely (with a beating frequency of approximately 10 GHz) in the hydrated layer of solutions, suggesting that this resulted in a decreased contact angle of  $64^\circ$  comparing to native PS of  $77^\circ$ . MCF7 breast cancer cells cultured in Pluronic copolymers (1% F108) formed multicellular spheroids, similar to those found in mammospheres except no supplementary mitogen used in this study, whereas cells cultured on traditional tissue culture dishes formed typical 2D monolayers (Figure 10c). In addition, we prepared Pluronic F108 of different concentrations coated onto PS dishes and then determined that 1% F108 was the optimal polymer for multicellular aggregate cultures and steric repulsion of hydrophobic molecules/proteins (Figure 11).

Notably, results from Figure 2b indicate that PS's hydrophobic nature tends to absorb small hydrophobic molecules in culture medium and might decrease the water contact angle as well as lower polymer coating (0.01% and 0.1% F108). In contrast, 1% F108-coated PS would efficiently prevent the absorption of molecules and proteins, thereby it has the capacity for 3D spheroid cultures to diminish cell-to-substrate adhesion. Similar to MCF7 and SKOV3 cells, human pancreatic cancer cell line (Panc 02.03B) and two human colorectal cancer cell lines (DLD-1 and SW480) all formed

multicellular spheroids in 1% F108 as well. The biomimetic nano-cilia by Pluronic F108 thus have potential to achieve modeling of tumor spheroids *in vitro*.



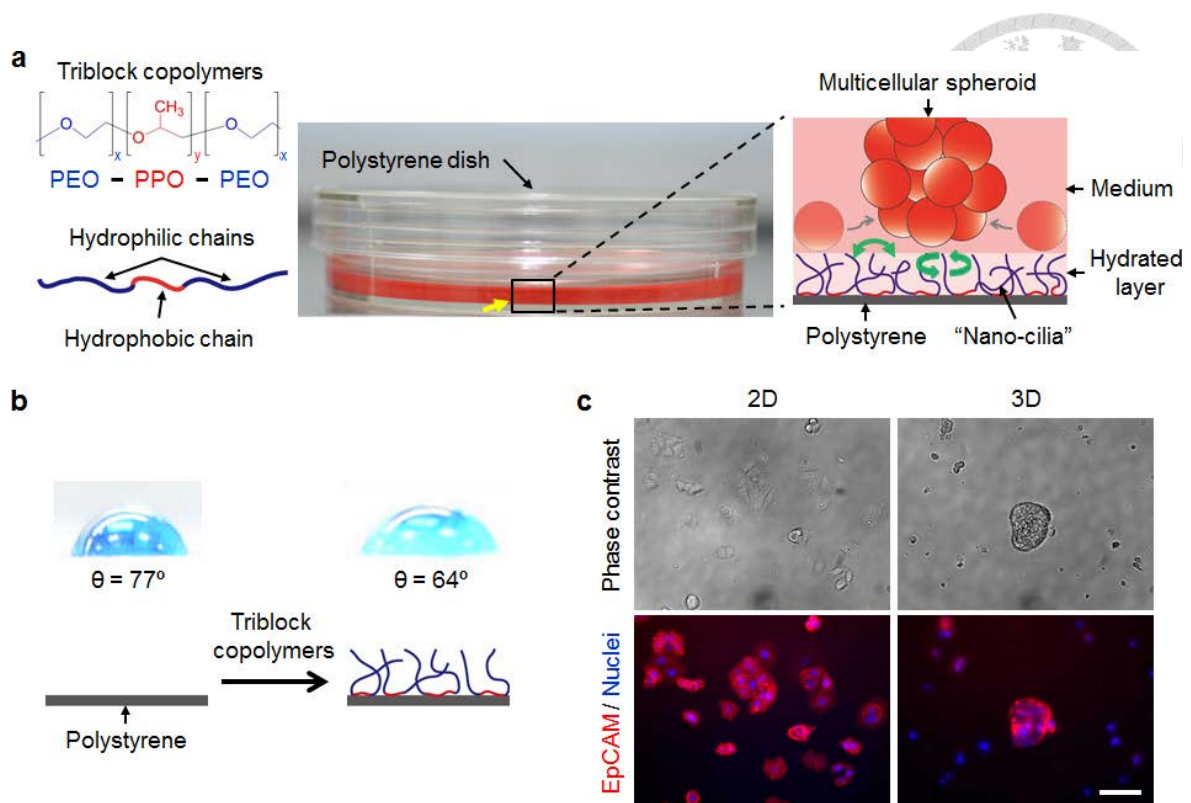


**Figure 10 3D spheroid cultured with triblock-copolymer (nano-cilia)-based locomotion.** *a*, Illustrations showing the configuration of the triblock copolymers (nano-cilia) system utilized for 3D multicellular spheroid cultures, in which  $x$  and  $y$  indicate the monomer units. Through the hydrophobic-hydrophobic interaction, the hydrophobic PPO chains will bind onto the PS surface and then beat the hydrophilic PEO chains freely in medium, thereby diminishing the cell-to-substrate adhesion and directing cell-cell interactions to organize a cellular spheroid. *b*, DI water drop with blue dye on PS surface before and after treatment with copolymers (1% Pluronic F108). A contact angle change of  $13^\circ$  was observed. *c*, Morphology of MCF7 cells cultured in conventional 2D monolayers and 3D spheroids as shown by phase contrast (top panel) and immunofluorescence (bottom panel; cell adhesion molecule stained with EpCAM, nuclear with Hoechst) images. Scale bar,  $100 \mu\text{m}$ .

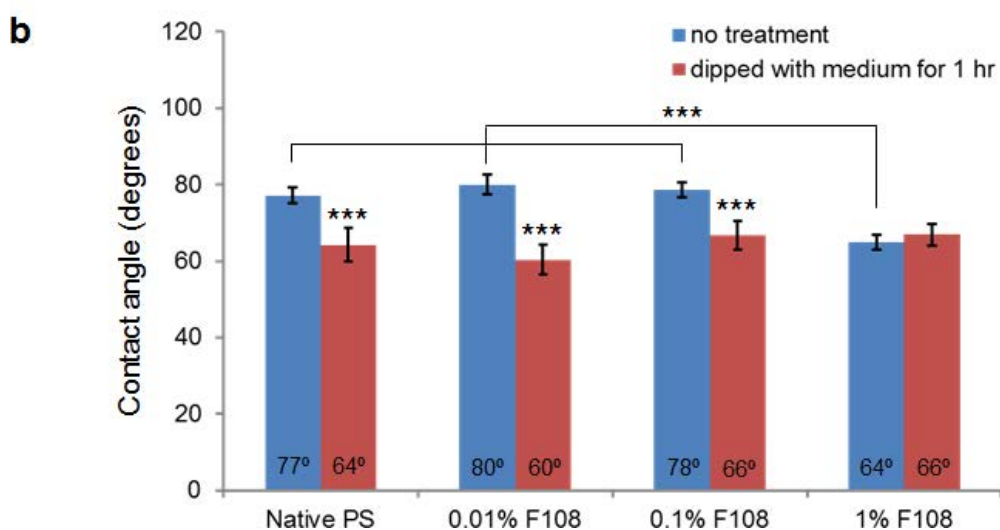
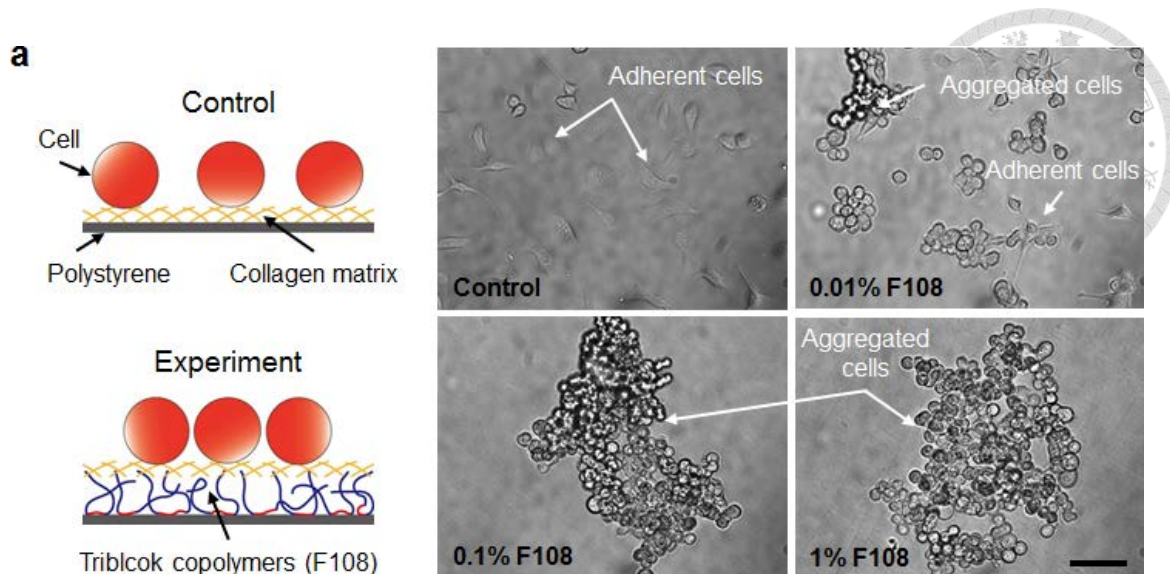


**Figure 11 Characteristics of triblock copolymers in steric repulsion.** (a) SKOV3 monolayer was cultured in collagen gel (100  $\mu\text{g}/\text{ml}$ )-coated PS surface (control), whereas multicellular aggregates were generated after one day culture in triblock copolymers of different concentrations (experiment). Scale bar, 100  $\mu\text{m}$ . (b) Comparison of contact angles on native and copolymer-coated PS surfaces. Colors in blue and red represent the surfaces without any treatment and by dipping in cell culture medium for 1 h, respectively. Contact angles were measured by dripping of a 1  $\mu\text{L}$  droplet of DI water on the PS surfaces. The data are presented as mean  $\pm$  SD from three independent experiments (\*\*\*)  $p < 0.001$ .

## Experimental methods to study tumor cell migration



**Micropipette assay:** a pipette is placed in the vicinity of the cell and a chemoattractant solution is injected into the culture medium establishing a growth-factor gradient.

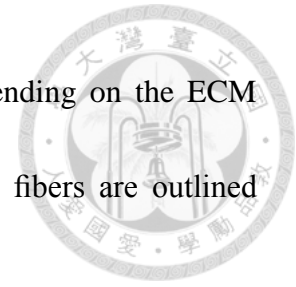
**Boyden (or Trans-well) chamber :** cells are seeded in suspension in the top chamber and migrate through the porous filter in response to a chemokine gradient, which is established by the different culture medium concentrations in the top and bottom chambers.

**Micropatterning:** cells are seeded on patterns of different geometry, size and surface coatings and their migration characteristics are monitored.

**Durotaxis:** cells are seeded on a substrate of variable stiffness and respond by changing traction forces, cell spread area, and migration direction.

**Wound healing:** a “wound” is formed on a confluent tumor monolayer, and the wound closure dynamics are monitored.

**3D ECM:** cells are seeded inside the 3D ECM and migrate depending on the ECM architecture (stiffness, pore size, and ligand concentration); ECM fibers are outlined with black curved lines.



**Microfluidics:** cytokine gradients can be established in a 3D matrix by flowing different chemokine concentration solutions in the left and right microchannels; Interstitial flow can be established by adjusting the hydrostatic pressure in the left and right microchannels; streamlines are indicated with dark magenta lines. Micropipette, Boyden chamber and microfluidics assays enable control of biochemical gradients. Durotaxis, 3D ECM and microfluidics assays enable control of biophysical forces (ECM stiffness and interstitial flow). Wound healing and micropatterning assay enable control of intercellular distances, whereas only micropatterning assays enable control of substrate topography. The schematics of each method are showed in Fig. 12, and the advantages/limitations of each method are summarized in Table 1.

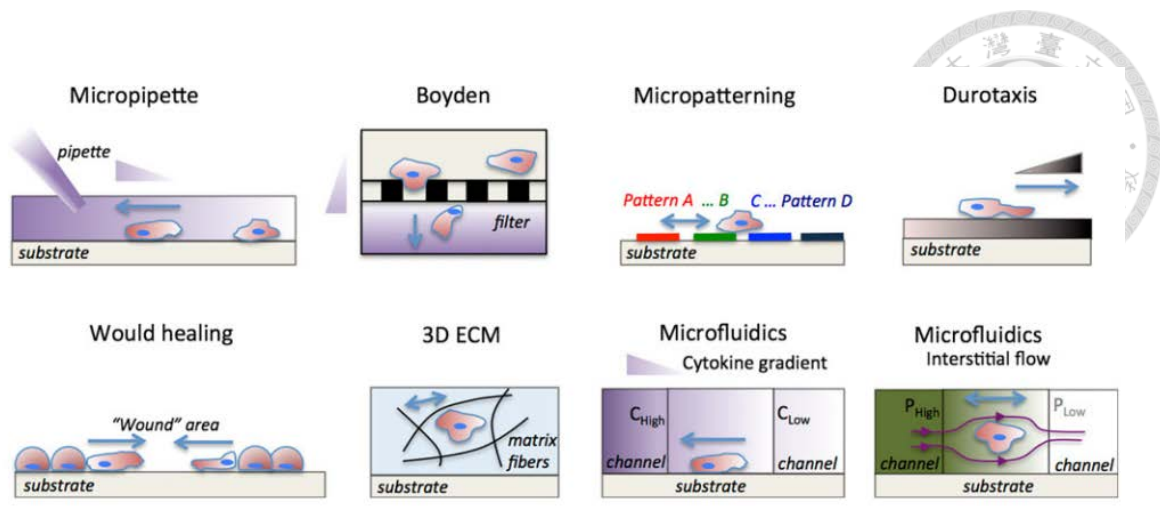


*Figure 12 Experimental methods for investigating factors that influence tumor cell migration.*

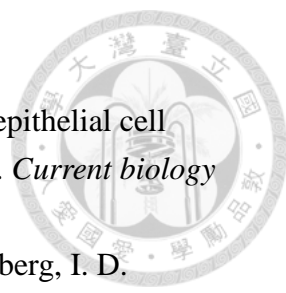
**Table 1** Comparison of *in vitro* experimental approaches to study tumor cell migration

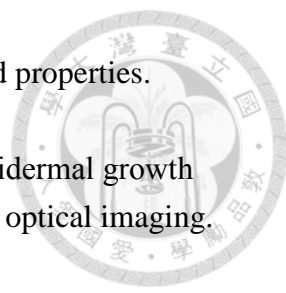
Assay	Key advantages/ disadvantages	Applications	Important parameters that can be controlled	Implementation guidelines
Transwell system or Boyden chamber	+High throughput +Easy to use –Live imaging –Gradient control –Cell population	Single and collective cell migration Co-culture of 2 cell types	Pore filter and protein coating characteristics, Chemoattractant to stimulate chemotaxis	No special equipment (commercially available, e.g., Corning, BD Biosciences)
Wound healing	+High throughput +Live imaging –2D substrate –Gradient control requires modifications	Collective cell migration	Wound area Substrate coating	No special equipment (commercially available, e.g., Essen BioScience)
Durotaxis assay	+Live imaging –2D substrate	ECM control	ECM coating ECM stiffness	Polyacrylamide substrates (Bio-Rad)
Micropipette	+Local stimulation +Live imaging –2D substrate –Low throughput –Temporal gradient decay	Chemotaxis Axon guidance	Injection parameters Substrate coating	Special equipment (micromanipulator, e.g., Narishige)
3D ECM	+Cell-ECM signaling –Confocal imaging –Gradient control requires modifications	EMT Tumor spheroid Proteolytic migration	ECM concentration (pore size, stiffness, ligand density) ECM layer thickness	Commercially available matrices (e.g., BD Biosciences)
Micropatterned	+Cell–cell signaling +Easy to use +Live imaging –Low cell numbers –Gradient control requires modifications	ECM topography Cell–cell interactions	Pattern dimensions Pattern coating	Microstencil, custom designs require wafer master (Stanford Microfluidic Foundry) and nanoimprint lithography (Scivax)
Microfluidic	+Fluid flow +Gradients +Cell–cell signaling +Live imaging –Complex to use –Low cell number –Biochemical assays	Microenvironment Temporal control of input signals	Flow-rate Gradients	Custom designs require wafer master (Stanford Microfluidic Foundry) Special equipment (syringe pumps: e.g., Harvard Apparatus; plasma cleaner: e.g., Harrick Plasma) Commercial microchannels (Ibidi, Millipore)

## Reference



- 1 Marx, V. Tracking metastasis and tricking cancer. *Nature* **494**, 133-138 (2013).
- 2 Kirby, B. J. *et al.* Functional characterization of circulating tumor cells with a prostate-cancer-specific microfluidic device. *PLoS One* **7**, e35976 (2012).
- 3 Chung, S. *et al.* Cell migration into scaffolds under co-culture conditions in a microfluidic platform. *Lab on a Chip* **9**, 269-275 (2009).
- 4 Kalchman, J. *et al.* A three-dimensional microfluidic tumor cell migration assay to screen the effect of anti-migratory drugs and interstitial flow. *Microfluidics and Nanofluidics*, 1-13 (2012).
- 5 Gurski, L. A., Petrelli, N. J., Jia, X. & Farach-Carson, M. C. 3D matrices for anti-cancer drug testing and development. *Oncology Issues* **25**, 20-25 (2010).
- 6 Becker, J. L. & Blanchard, D. K. Characterization of primary breast carcinomas grown in three-dimensional cultures. *Journal of Surgical Research* **142**, 256-262 (2007).
- 7 David, L. *et al.* Hyaluronan hydrogel: an appropriate three-dimensional model for evaluation of anticancer drug sensitivity. *Acta biomaterialia* **4**, 256-263 (2008).
- 8 Horning, J. L. *et al.* 3-D tumor model for in vitro evaluation of anticancer drugs. *Molecular pharmaceutics* **5**, 849-862 (2008).
- 9 Friedl, P., Zänker, K. S. & Broecker, E.-B. Cell migration strategies in 3-D extracellular matrix: differences in morphology, cell matrix interactions, and integrin function. *Microscopy research and technique* **43**, 369-378 (1998).
- 10 Cukierman, E., Pankov, R., Stevens, D. R. & Yamada, K. M. Taking cell-matrix adhesions to the third dimension. *Science* **294**, 1708-1712 (2001).
- 11 Friedl, P. & Bröcker, E.-B. The biology of cell locomotion within three-dimensional extracellular matrix. *Cellular and molecular life sciences CMLS* **57**, 41-64 (2000).
- 12 Liang, C.-C., Park, A. Y. & Guan, J.-L. In vitro scratch assay: a convenient and inexpensive method for analysis of cell migration in vitro. *Nature protocols* **2**, 329-333 (2007).
- 13 Kam, Y., Guess, C., Estrada, L., Weidow, B. & Quaranta, V. A novel circular invasion assay mimics in vivo invasive behavior of cancer cell lines and distinguishes single-cell motility in vitro. *BMC cancer* **8**, 198 (2008).
- 14 Su, P. *et al.* Epigenetic silencing of PTPRR activates MAPK signaling, promotes metastasis and serves as a biomarker of invasive cervical cancer. *Oncogene* **32**,

- 
- 15-26 (2012).
- 15 Omelchenko, T. & Hall, A. Myosin-IXA regulates collective epithelial cell migration by targeting RhoGAP activity to cell-cell junctions. *Current biology* **22**, 278-288 (2012).
- 16 Rosen, E. M., Meromsky, L., Setter, E., Vinter, D. W. & Goldberg, I. D. Quantitation of cytokine-stimulated migration of endothelium and epithelium by a new assay using microcarrier beads. *Experimental cell research* **186**, 22-31 (1990).
- 17 Harisi, R. *et al.* Differential inhibition of single and cluster type tumor cell migration. *Anticancer research* **29**, 2981-2985 (2009).
- 18 Qi, S. *et al.* ZEB2 mediates multiple pathways regulating cell proliferation, migration, invasion, and apoptosis in glioma. *PloS one* **7**, e38842 (2012).
- 19 Zhang, Q., Liu, T. & Qin, J. A microfluidic-based device for study of transendothelial invasion of tumor aggregates in realtime. *Lab on a chip* **12**, 2837-2842 (2012).
- 20 Bockhorn, M., Roberge, S., Sousa, C., Jain, R. K. & Munn, L. L. Differential gene expression in metastasizing cells shed from kidney tumors. *Cancer research* **64**, 2469-2473 (2004).
- 21 Vernon, R. B. & Gooden, M. D. New technologies in vitro for analysis of cell movement on or within collagen gels. *Matrix biology* **21**, 661-669 (2002).
- 22 Yarrow, J. C., Totsukawa, G., Charras, G. T. & Mitchison, T. J. Screening for cell migration inhibitors via automated microscopy reveals a Rho-kinase inhibitor. *Chemistry & biology* **12**, 385-395 (2005).
- 23 Tung, Y.-C. *et al.* High-throughput 3D spheroid culture and drug testing using a 384 hanging drop array. *Analyst* **136**, 473-478 (2011).
- 24 Yu, L., Chen, M. C. & Cheung, K. C. Droplet-based microfluidic system for multicellular tumor spheroid formation and anticancer drug testing. *Lab on a Chip* **10**, 2424-2432 (2010).
- 25 Wu, L. Y., Di Carlo, D. & Lee, L. P. Microfluidic self-assembly of tumor spheroids for anticancer drug discovery. *Biomedical microdevices* **10**, 197-202 (2008).
- 26 Burgess, B. T., Myles, J. L. & Dickinson, R. B. Quantitative analysis of adhesion-mediated cell migration in three-dimensional gels of RGD-grafted collagen. *Annals of biomedical engineering* **28**, 110-118 (2000).
- 27 Abhyankar, V. V. *et al.* A platform for assessing chemotactic migration within a spatiotemporally defined 3D microenvironment. *Lab on a Chip* **8**, 1507-1515 (2008).
- 28 Yu, D. *et al.* c-erbB-2/neu overexpression enhances metastatic potential of

- 
- human lung cancer cells by induction of metastasis-associated properties. *Cancer research* **54**, 3260-3266 (1994).
- 29 Thorne, R. G., Hrabětová, S. & Nicholson, C. Diffusion of epidermal growth factor in rat brain extracellular space measured by integrative optical imaging. *Journal of neurophysiology* **92**, 3471-3481 (2004).
- 30 Bernards, R. & Weinberg, R. A. Metastasis genes: a progression puzzle. *Nature* **418**, 823-823 (2002).
- 31 Pantel, K., Cote, R. J. & Fodstad, Ø. Detection and clinical importance of micrometastatic disease. *Journal of the National Cancer Institute* **91**, 1113-1124 (1999).
- 32 Dontu, G. *et al.* In vitro propagation and transcriptional profiling of human mammary stem/progenitor cells. *Genes Dev.* **17**, 1253-1270 (2003).
- 33 Pickl, M. & Ries, C. H. Comparison of 3D and 2D tumor models reveals enhanced HER2 activation in 3D associated with an increased response to trastuzumab. *Oncogene* **28**, 461-468 (2009).
- 34 Friedrich, J., Seidel, C., Ebner, R. & Kunz-Schughart, L. A. Spheroid-based drug screen: considerations and practical approach. *Nature Protocols* **4**, 309-324 (2009).
- 35 Sharma, S. V., Haber, D. A. & Settleman, J. Cell line-based platforms to evaluate the therapeutic efficiency of candidate anticancer agents. *Nat. Rev. Cancer* **10** (2010).
- 36 Chen, L. *et al.* The enhancement of cancer stem cell properties of MCF-7 cells in 3D collagen scaffolds for modeling of cancer and anti-cancer drugs. *Biomaterials* **33**, 1437-1444 (2012).